

Optothermal response and Tissue Damage analysis during Laser Hair Removal

Micheal O. Okebiorun and Sherif H. ElGohary
Department of Biomedical Engineering and Systems,
Faculty of Engineering, Cairo University.
Cairo, Egypt

Email: Sh.ElGohary@eng1.cu.edu.eg

Abstract. Effective design of laser sources is crucial to optimum performance during Laser hair removal. Therefore, the thermal effect of laser sources was evaluated at wavelengths 694, 755, and 1064 nm at different fluence 4.5, 5.5, 10, and 15 J/cm², respectively. The patient skin models are 3 photo types of a 3-layer 3D model of epidermis, dermis and hypodermis containing the hair shaft and follicle with thickness carefully selected to be in range of a normal human feature. Monte Carlo method, Bio heat transfer and thermal damage analysis using Arrhenius formula were employed. Results show that a laser source of 10-15 J/cm², at 755 nm wavelength is optimal for light skinned and moderate skinned while 4.5 -10 J/cm², 755-1064 nm is optimal for dark skinned people for a pulse width of 0.1 sec. This work would assist researchers and manufacturers in the design and development of hair photoepilation devices.

Keywords—laser hair removal, thermal damage, skin-type, Monte Carlo.

1. Introduction

Artificial hair removal is now a very common practice in many walks of life. Most people undergo this activity regularly due to various reasons such as religious, cultural, medical, social, sports and psychological reasons [1]. Unwanted hair growth can have an adverse psychological effect especially environments with a bias for this. Although, hair can be considered an aesthetic feature in man, growth of hair on certain regions in the body can be considered abnormal or not fit for the society or his personality or activities.

Over the years, various techniques have been developed for removal of hair. Current practices include waxing, chemical depilatories, electrolysis, threading and the traditional shaving technique. Drawbacks of these techniques include pain, limitation as regards hair length, skin irritation, wounds and so on [1]–[3]. Removal of hair using laser technology which has become very popular is argued by various studies to be the most efficient method [1], [3]–[6]. This technique is basically the photothermal destruction of hair follicles with red and near-infrared wavelengths suitable for targeting follicular and hair shaft melanin using any of these laser sources; normal mode ruby laser (694 nm), normal mode alexandrite laser (755 nm), pulsed diode lasers (800, 810 nm), long-pulse Nd:YAG laser (1,064 nm), and intense pulsed light (IPL) sources (590-1,200 nm) [1]. Specifically, regarding IPL-based treatment, Godfrey et al made a review of articles on this and showed that a single low fluence pulse of both 810 nm laser (6.6 J/cm², 16ms) and IPL (9 J/cm², 15ms and 6.8 J/cm², 1.9ms) leads to induction of catagen transition which is expected to eventually lead to hair reduction[7]. It was also demonstrated home-use IPL



appliances can cause persistent hair reduction up to one year after treatment [7]. There are variations in the optical properties of different skin photo types which also elicit different responses to different laser spectral. This is due to the varying melanin content which also accounts for skin color variation. It is expected that sufficient heat is delivered to hair follicles to thermally destroy it and also to for good confinement to prevent permanent thermal damage to non-targeted skin. Therefore, there is need for research into laser parameters for optimal performance for each skin type.

Most studies have been conducted on light skin type (Fitzpatrick I & II). For example, Ataie-Fashtami et al investigated the heat distribution and thermal damage on a single hair strand during laser hair removal at different pulse widths using the LITCIT software [8]. However, the analysis was only carried out for a single skin (Fitzpatrick II) and hair type while they also do not provide the fluence distribution. On the other hand, it has also been widely known that lasers can also be used for the opposite effect, that is, improving the growth of hair or the treatment of Androgenetic Alopecia (AGA). Ratchathorn et al identified the proteome set which implicates this process as discussed here [9].

Researchers have analyzed laser-tissue responses with various simulation tools and theories. Monte Carlo method, a class of computational algorithms which rely on repeated random sampling to deliver numerical results has proven to be extremely valuable in solving probabilistic problems. Since, the light distribution is considered a highly probabilistic distribution, this computational tool is therefore employed in simulating the distribution of photons in many studies [10].

Furthermore, Light-based treatments are usually accompanied by desired or unwanted temperature change which is very crucial to the accuracy and safety of these procedures. In this procedure, it is important to have a foreknowledge of the accompanying heat generated. Researchers usually employ a finite element thermal model via the bio-heat equation to describe this kind of heat transfer. For example, a study employed the bio-heat equation to obtain the temperature distribution during hair removal and also employed the Arrhenius formula to obtain the accompanying thermal damage [8].

In this study, we developed 3D models of a 3-layer skin for 3 skin types with an array of hair, investigated and compared light and temperature distribution based on 3D Monte Carlo method and the bio-heat equation in the models at 3 different wavelengths and at 4 different power. Most importantly, we evaluated the thermal damage caused to in the skin tissues with different laser sources.

2. Results

The results of the Monte Carlo simulation provide the energy distribution of light, as a way to forecast the influence of light on a model based on real parameters for a safe and effective laser hair removal. The temperature distributions obtained from the bio heat transfer equation are also presented while the thermal damage obtained from the Arrhenius formula are also explained.

Figure 1 shows the entire fluence distribution for the 3 skin types which show the difference in absorption in these photo types at wavelength 755 nm and 5.5 J/cm² energy source. The depth of all our models is 8 mm into the skin as shown in the figures. For the light skin type, most portion of the light energy is transmitted down to the dermal layer while for the dark skin type, most of the light is being absorbed at the epidermal layer.

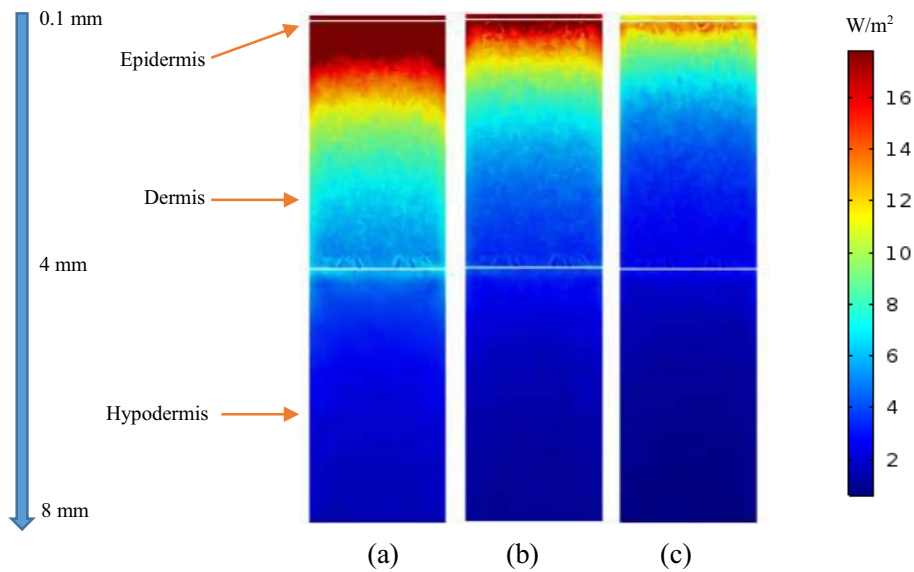


Fig. 1 Fluence distribution (W/m^2) for (a) light (b) moderate (c) dark skin types for wavelength 755 nm and $5.5 J/cm^2$

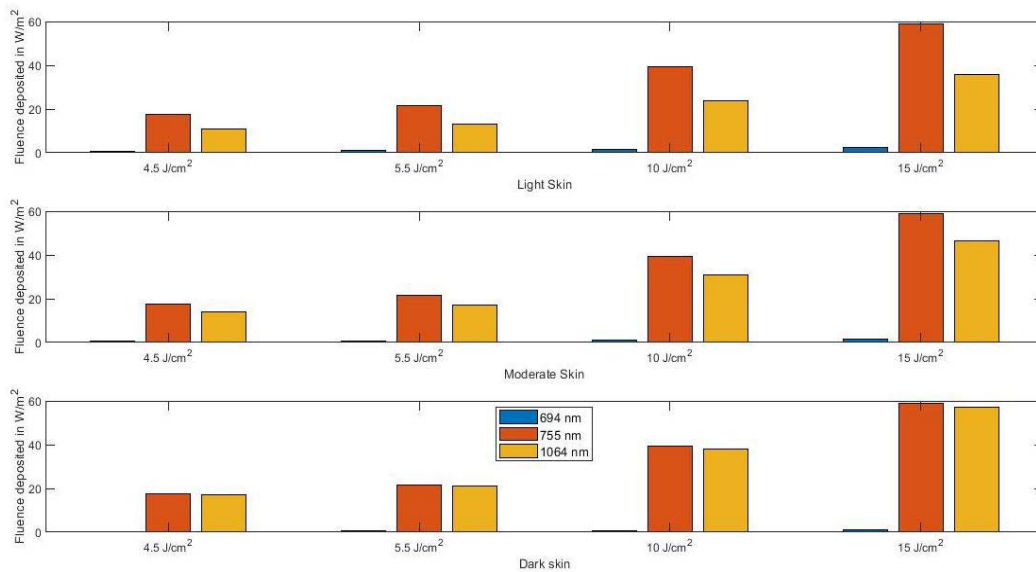


Fig. 2 Fluence deposited at the base of the hair follicle for all skin types at wavelengths 694, 755 and 1064 nm and at different energy sources.

Figure 2 reveals the fluence deposited at the base of the hair follicle for different laser source configurations. It shows maximum absorption at 755 nm wavelength for all skin types while very minimal absorption at 694 nm. For the dark skin, the difference between the effect of the 755 and 1064 nm laser source is not much compared to the effect for the light skin type.

Figure 3 compares the response of a dark skin at wavelengths 694, 755 and 1064 nm and energy source of $15 J/cm^2$. At this energy source, the temperature of the skin rises up to $300\text{ }^\circ\text{C}$ at 755 nm wavelength. For a 694 nm source, the temperature was between 160 and $180\text{ }^\circ\text{C}$ and for 1064 nm source, the temperature all through the model hovers between 210 and $230\text{ }^\circ\text{C}$.

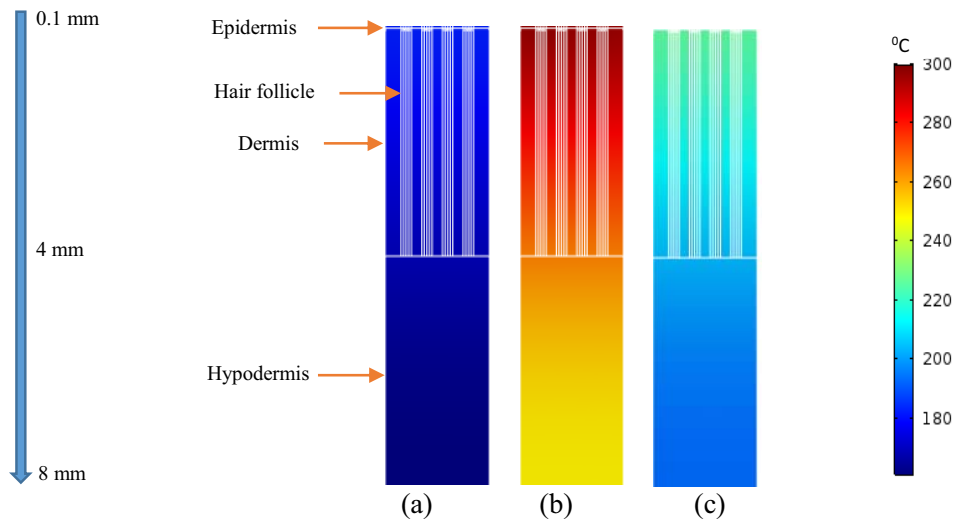


Fig. 3 Temperature distribution in degrees Celsius on the dark skin at (a) 694 (b) 755 (c) 1064 nm respectively with a laser source of 15 J/cm^2

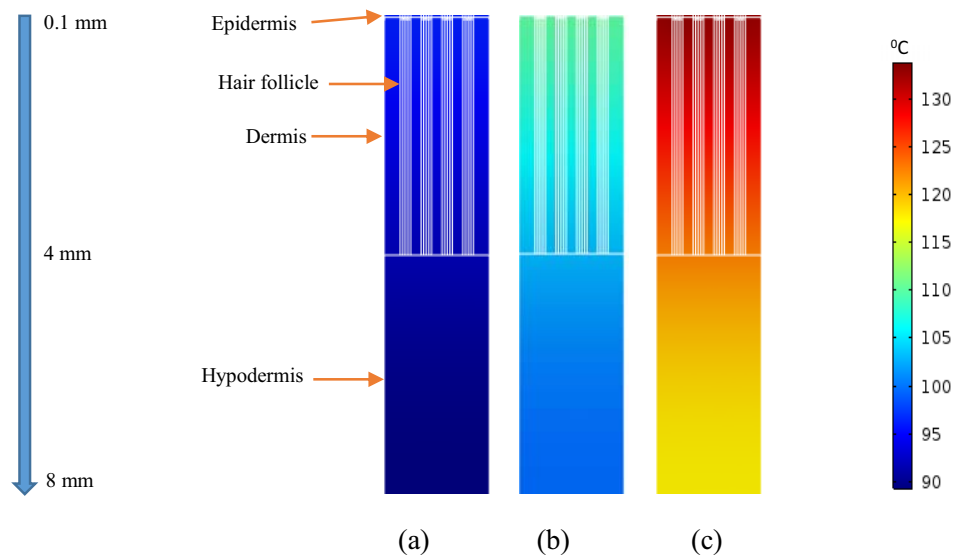


Fig. 4 Temperature distribution in degrees Celsius in (a) light (b) moderate (c) dark skin types at 755 nm and 5.5 J/cm^2

Figure 4 shows comparison between the three skin types at 755 nm and 5.5 J/cm^2 . With this laser configuration, the maximum temperature attained by the dark skin is at 134 degrees and the lowest temperature for this skin type is $117 \text{ }^\circ\text{C}$. However, for the light skin, it barely reaches 100 degrees.

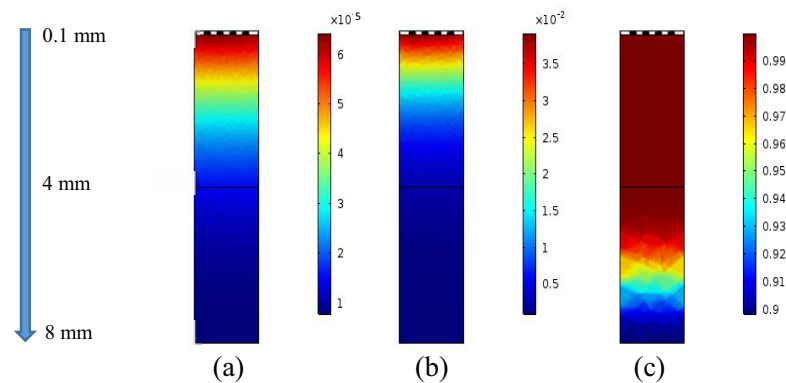


Fig. 5 Thermal damage distribution in (a) light (b) moderate (c) dark skin types at 694 nm and 4.5 J/cm²

For the thermal damage analysis, 10 and 15 J/cm² obtained for all models a damage integral of 1 while for temperature distribution below 60 °C, a damage integral of 0.00001-0.99 were obtained. Figure 5 shows the thermal damage for the 3 skin types at wavelength 694 nm and 4.5 J/cm² where the maximum possible value is 1 as obtained by equation 2.

3. Discussion

Figure 1 reveals that light is absorbed more in the dermal layer of the light skins which may result into high deposition of energy, a laser source with lower wavelength or energy is therefore necessary. While figure 2 also compares different laser configurations which reveals the response of each skin type to these laser source variations at the base of the hair follicle. It is observed that at 10-15 J/cm², much fluence is deposited in the skins which is a good idea for light skin but could cause a very high temperature change for dark skins, an adjustment in the wavelength or energy source is also therefore necessary. Localization of the fluence in the dermal layer is vital since the target tissue (hair follicle) is fully located in this region. The temperature distribution and the thermal damage analysis in figures 3, 4 and 5 indicate a clearer and quantitative results. Figure 3 shows that at 755 nm, more energy is deposited in the dermal layer and the temperature change was higher than the other wavelengths which indicates that 755 nm source is better than others. Figure 4, which shows the temperature change that accompanying the light distribution, suggests that for a more optimal temperature change, an energy source of more than 5.5 J/cm² is necessary especially for light and moderate skin type. In figure 5, it can be deduced that energy of more than 4.5 J/cm² is necessary to have an effective damage to the hair follicle at 694 nm wavelength. The dark skin however can attain 99 % damage at this energy source but the light and moderate skin are barely affected. Although, at temperature greater than 60 °C, the hair follicle cells begin to get weakened and dormant, it is necessary to reach about 100 degrees to achieve a permanent damage of the cells. Extreme temperatures such as >150 degrees also should be avoided so as to prevent irreversible damage to the dermal layer. Therefore, a laser source of 10-15 J/cm², 755 nm is optimal for light skinned and moderate skinned while 4.5 -10 J/cm², 755-1064 nm is optimal for dark skinned people for a pulse of 0.1s. These deductions about our dark-skinned model agree a review study by Rachel et al [11] while Ataie-Fashtami et al suggest for high fluence of 40 – 50 J/cm², 400ms for a 10 -mm spot size at 810 nm for moderately pigmented people [8], with spot-size adjustments, this also complies with our results. Although, external cooling was not factored into this study, this gives us yet a good view of what is expected for these configurations during laser hair removal. Experimental work is however necessary to confirm this work.

4. Material and Methods

TABLE 1. OPTICAL PROPERTIES OF THE SKIN LAYERS [8], [12]

Wavelength (nm)	Skin type I-II μ_a Epidermis (mm^{-1})	Skin type III-IV μ_a Epidermis (mm^{-1})	Skin type V-VI μ_a Epidermis (mm^{-1})	Skin type I-II μ_a Hair shaft (mm^{-1})	Skin type III-IV μ_a Hair shaft (mm^{-1})	Skin type V-VI μ_a Hair shaft (mm^{-1})	Dermis μ_a (mm^{-1})	Scattering coefficient μ_s (mm^{-1})	Anisotropy Factor g	Refractive Index
694	0.709	2.990	6.860	1.0	3.5	8.0	0.275	5	0.87	1.37
755	0.541	2.260	5.180	0.7	2.67	7.0	0.263	5	0.87	1.37
1064	0.189	0.736	1.667	0.5	1.05	2.0	0.259	5	0.87	1.37

A. Modelling of the various skin photo types

The 3D proposed patient skin models consists of a 3-layers epidermis, dermis and hypodermis containing the hair shaft and follicle with thickness carefully selected to be in range of a normal human feature. The skin is a 2 x 2 mm layers of hypodermis (4mm), dermis (3.9 mm), epidermis (0.1 mm), hair follicle (0.2 mm radius, 4 mm depth), hair shaft (0.1 mm radius and 4mm depth).

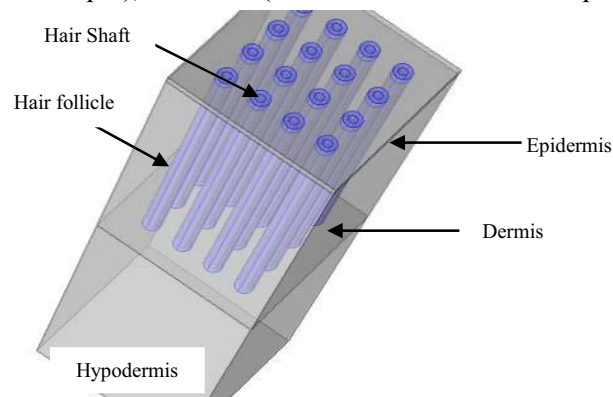


Fig. 6 The Skin model

Skin models (see Fig. 6) were modelled based on the optical properties in table 1, the epidermis and the hair follicle are assumed to have the same optical properties according to [7], the entire skin was assumed to have the same scattering coefficient, anisotropy factor and refractive index. The dermal and hypodermal layer are also assumed to have the same optical properties because the variations in the skin properties are due to melanin content which is localized in the epidermal layer and hairs. The light skin type represents the Fitzpatrick I & II, the moderate skin type represents the Fitzpatrick III & IV and the dark skin type represents the Fitzpatrick V & VI as expressed in Table 1.

B. Simulation of the fluence distribution in the skin tissues

In this study, 3×10^6 photons were simulated using the Monte Carlo Method with a 2 x 2 mm laser source placed on the skin surface. Fluence of 4.5, 5.5, 10 and 15 J/cm^2 were employed at wavelengths 694, 755 and 1064 nm. Light distribution was estimated based on 3D Monte Carlo technique. This is a

stochastic technique, which rely on repeated random sampling to deliver numerical results. Implementation of this algorithm for our study was carried out with the Molecular Optical Simulation Environment (MOSE) software as described somewhere else [14].

C. Temperature change distribution in the models

The temperature change in our skin models was described by bio-heat equation in an FE simulator as shown below [8].

$$\rho C \frac{\partial T}{\partial t} - \nabla \cdot (k \nabla T) = Q \quad (1)$$

Where ρ is the density, C is the specific heat capacity, k is the thermal conductivity and T is the temperature in Celsius. Q is the heat source in W/m^3 obtained from the multiplication of μ_a and Φ from the light propagation procedure above. Heat generated as a result of biological processes are ignored since the temperature change desired is due to the external input. This equation was used to generate the temperature distribution in the skin models

TABLE 2 THERMAL PROPERTIES OF THE MODEL [7]

Parameter	Epidermis	Dermis	Hair follicle	Shaft
Density (ρ)	1.1497	1.075	1.1497	1.1497
Specific Heat Capacity C (J/kg/K)	2.789	3.488	2.789	2.789
Thermal Conductivity k (W/m.k)	0.0034	0.0048	0.0034	0.0034

C. Thermal damage in the hair follicle

In our simulation, we investigated whether the laser source is sufficient to completely destroy the hair follicle so as to prevent further hair growth so as to not to cause any irreversible damage to the surrounding tissue. This can be described by the Arrhenius formula which calculates the state of protein denaturation as a rate equation [8]. This was used in our analysis to obtain the thermal damage to the tissues.

$$\Omega(T, t) = A \int_{t_i}^{t_f} \exp\left(\frac{-E}{RT}\right) dt \quad (2)$$

$\Omega(T, t)$ is the damage integral, R is the universal gas constant ($8.314 J/mol.K$), t is the time of irradiation, and A and E are the Arrhenius constants with values of ($3.1 \times 10^{98} s^{-1}$) and ($6.3 \times 10^5 J/mol$) respectively.

5. Conclusion

This study shows the light distribution in the skin, temperature distribution in the hair follicles and effectual thermal damage to the follicles. Specifically, our simulation clearly reveals the light energy distribution for light, moderate and dark-skin models which correspond to Fitzpatrick I & II, III & IV and V & VI skin types respectively at 694, 755, 1064 nm and 4.5, 5.5, 10, 15 J/cm^2 energy sources for this medical procedure. that a laser source of 10-15 J/cm^2 , at 755 nm wavelength is optimal for light skinned and moderate skinned while 4.5 -10 J/cm^2 , 755-1064 nm is optimal for dark skinned people for a pulse width of 0.1 sec. We intend to expand our work on this idea especially in the temperature distribution factoring in external cooling and metabolic processes, and further explore the detection of precise skin optical properties using deep learning algorithms in the epidermal layer of the skin. This

study will therefore assist researchers and manufacturers on development of equipment for laser hair removal.

REFERENCES

- [1] M. Haedersdal and C. S. Haak, "Hair Removal," in *Current problems in dermatology*, vol. 42, 2011, pp. 111–121.
- [2] D. Shi, Y. Yao, and W. Yu, "Comparison of preoperative hair removal methods for the reduction of surgical site infections: a meta-analysis," *J. Clin. Nurs.*, vol. 26, no. 19–20, pp. 2907–2914, Oct. 2017, doi: 10.1111/jocn.13661.
- [3] D. K. Paras Vakharia, Dirk M Elston, "Nonlaser Hair Removal Techniques: Overview, Temporary Hair Removal, Temporary Hair Reduction," *Medscape*, 2016. [Online]. Available: <https://emedicine.medscape.com/article/1067139-overview>. [Accessed: 03-Jun-2018].
- [4] M. Haedersdal and H. Wulf, "Evidence-based review of hair removal using lasers and light sources," *J. Eur. Acad. Dermatology Venereol.*, vol. 20, no. 1, pp. 9–20, Jan. 2006, doi: 10.1111/j.1468-3083.2005.01327.x.
- [5] U. A. Patil and L. D. Dhami, "Overview of lasers.," *Indian J. Plast. Surg.*, vol. 41, no. Suppl, pp. S101-13, Oct. 2008.
- [6] E. A. Olsen, "Methods of hair removal," *J. Am. Acad. Dermatol.*, vol. 40, no. 2, pp. 143–155, Feb. 1999, doi: 10.1016/S0190-9622(99)70181-7.
- [7] G. Town *et al.*, "Light-based home-use devices for hair removal: Why do they work and how effective they are?," *Lasers in Surgery and Medicine*, vol. 51, no. 6. John Wiley and Sons Inc., pp. 481–490, 01-Aug-2019, doi: 10.1002/lsm.23061.
- [8] L. Ataie-Fashtami *et al.*, "Simulation of Heat Distribution and Thermal Damage Patterns of Diode Hair-Removal Lasers: An Applicable Method for Optimizing Treatment Parameters," *Photomed. Laser Surg.*, vol. 29, no. 7, pp. 509–515, Jul. 2011, doi: 10.1089/pho.2010.2895.
- [9] R. Panchaprateep, T. Pisitkun, and N. Kalpongkul, "Quantitative proteomic analysis of dermal papilla from male androgenetic alopecia comparing before and after treatment with low-level laser therapy," *Lasers Surg. Med.*, vol. 51, no. 7, pp. 600–608, 2019, doi: 10.1002/lsm.23074.
- [10] S. H. El-Gohary, M. K. Metwally, S. Eom, S. H. Jeon, K. M. Byun, and T.-S. Kim, "Design study on photoacoustic probe to detect prostate cancer using 3D Monte Carlo simulation and finite element method," *Biomed. Eng. Lett.*, vol. 4, no. 3, pp. 250–257, Sep. 2014, doi: 10.1007/s13534-014-0150-2.
- [11] R. A. Fayne, M. Perper, A. E. Eber, A. S. Aldahan, and K. Nouri, "Laser and Light Treatments for Hair Reduction in Fitzpatrick Skin Types IV–VI: A Comprehensive Review of the Literature," *Am. J. Clin. Dermatol.*, vol. 19, no. 2, pp. 237–252, Apr. 2018, doi: 10.1007/s40257-017-0316-7.
- [12] "Skin Optics Summary." [Online]. Available: <https://omlc.org/news/jan98/skinoptics.html>. [Accessed: 10-Sep-2019].
- [13] L. Ataie-Fashtami *et al.*, "Simulation of Heat Distribution and Thermal Damage Patterns of Diode Hair-Removal Lasers: An Applicable Method for Optimizing Treatment Parameters," *Photomed. Laser Surg.*, vol. 29, no. 7, pp. 509–515, Jul. 2011, doi: 10.1089/pho.2010.2895.
- [14] S. Ren *et al.*, "Molecular Optical Simulation Environment (MOSE): A Platform for the Simulation of Light Propagation in Turbid Media," *PLoS One*, vol. 8, no. 4, p. e61304, Apr. 2013, doi: 10.1371/journal.pone.0061304.